Science of the Total Environment 743 (2020) 140604

Contents lists available at ScienceDirect

Science of the Total Environment

journal homepage: www.elsevier.com/locate/scitotenv

Biochar as composite of phosphate fertilizer: Characterization and agronomic effectiveness

Denison Pogorzelski [a,*], José Ferreira Lustosa Filho [a], Patrícia Cardoso Matias [a], Wedisson Oliveira Santos [b], Leonardus Vergütz [a,d], Leônidas Carrijo Azevedo Melo [c]

[a] Department of Soils, Federal University of Viçosa, 36570-900 Viçosa, MG, Brazil
[b] Institute of Agrarian Science, Federal University of Uberlândia, 38400-000 Uberlândia, MG, Brazil
[c] Department of Soil Science, Federal University of Lavras, 37200-900 Lavras, MG, Brazil
[d] Mohammed VI Polytechnic University (UM6P), Benguerir 43150, Morocco

HIGHLIGHTS

- Organomineral phosphate fertilizer (OMP) was produced by blending or coating triple superphosphate (TSP) with biochar (BC).
- Kinetics of P release and effectiveness agronomic of OMPs and TSP were assessed.
- OMPs have lower P release when compared with TSP.
- Biochar coating is more effective than blending to reduce P release in OMP.
- OMP promoted higher P recovery rate and plant P uptake than TSP in the clayey soil.

GRAPHICAL ABSTRACT

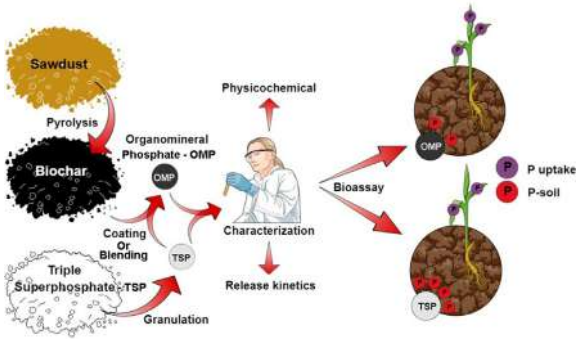

ARTICLE INFO

Article history:
Received 2 April 2020
Received in revised form 26 June 2020
Accepted 27 June 2020
Available online 29 June 2020

Editor: Daniel CW Tsang

Keywords:
Organomineral phosphate fertilizer
P release kinetics
Slow release fertilizer
P use efficiency

ABSTRACT

Organomineral phosphate fertilizers (OMP) may reduce phosphate release rate and its direct contact to the soil solid phase, increasing the effectiveness of phosphorus (P) fertilization. This study aimed to evaluate the effect of granulating biochar (BC) with triple superphosphate (TSP) in two forms (blend or coated) and three proportions (5, 15 and 25%, w/w) on the P release kinetics and plant growth. A successive plant trial using two soils of contrasting P buffering capacities and five P doses (0, 20, 40, 80 and 120 mg kg^{-1}) was set to investigate the agronomic effectiveness of OMP that presented the slowest P release kinetic. The kinetic test showed that within the first 1.5 h, TSP, OMP blend and OMP coated fertilizers released 92, 82 and 36% of total P, respectively. Thereby, BC addition to TSP reduced the P release rate, mainly due to coating. The fertilizers coated with 15% and 25% BC (C15 and C25, respectively) presented the slowest P release rate. For the plant trial, C15 was chosen because it requires less BC when compared with C25 fertilizer. In the first crop, C15 provided more P to plants, especially in the soil with high P buffering capacity, which increased by 10% and 20% the P uptake and the P recovered by the plant when compared with TSP, respectively. In the sandy soil, fertilizers C15 and TSP showed the same performances regarding yield, P uptake and P recovery rate. At consecutive cultivation, regardless of the soil type, P sources (C15 and TSP) did not differ in yield, P uptake and P recovery. Therefore, biochar-based organomineral phosphate fertilizer can enhance P use efficiency in high P-fixing tropical soils, increasing P recovery and uptake when compared with TSP.

* Corresponding author.
E-mail address: denison.pogorzelski@ufv.br (D. Pogorzelski).

https://doi.org/10.1016/j.scitotenv.2020.140604
0048-9697/

1. Introduction

Highly weathered tropical soils have high capacity of P sorption due to the presence of high contents of Al—Fe oxyhydroxides (goethite, hematite, gibbsite) and kaolinite in the clay fraction (Campos et al., 2016; Gérard, 2016). In fact, functional groups present on the surface of these minerals (-AlOH, -FeOH) have high chemical affinity with orthophosphate, leading to high-energy coordinate bonds and fast reactions. Therefore, in these conditions most part of added P as highly water-soluble fertilizers becomes unavailable to plants, leading to a low P recovery by plants and a low efficiency of phosphate fertilization (Roy et al., 2017). Consequently, heavy and recurrent P fertilizations are required to ensure crop yields, increasing the cost of production and reducing the efficiency in the use of phosphate rock, which is a finite and non-renewable resource (Baveye, 2015; Gilbert, 2009; Roy et al., 2016). Facing the low efficiency of P-fertilization in humid tropical conditions, "*smart fertilizers*" emerge as a potential alternative aiming to increase the sustainability of P use in tropical agriculture (Benício et al., 2017; Calabi-Floody et al., 2018; Lustosa Filho et al., 2017; Santos et al., 2019; Withers et al., 2015).

Biochar (BC) is the solid fraction obtained from pyrolysis of biomass under low or limited oxygen supply, which allows C retention in soils and helps mitigating CO_2 emissions to the atmosphere (Lehmann and Joseph, 2015). In Brazil, wood waste, which is produced in large quantities, is considered a biomass source that can be converted into BC and applied to soil causing an increase in C stock (Lora and Andrade, 2009). Furthermore, BC plays a role as soil amendment, improving soil quality (Dai et al., 2017; Novak et al., 2009). However, BC application rates of 15 t ha^{-1} (median value) in tropical soils are usually needed to significantly improve crop yield (Jeffery et al., 2017), which is unfeasible at large scale due to high costs. Conversely, combining BC with soluble P-fertilizers is an attractive strategy to reduce the P release rate allowing gradual application of BC to soil and being an environmentally friendly usage way of biomass.

Beyond the environmental benefits, BC has interesting characteristics to compose the fertilizer matrix, such as high porosity and functional surface groups that acts as adsorbent, especially those doped/modified (Jiang et al., 2018; Li et al., 2016a; Novais et al., 2018; Vikrant et al., 2018). Some studies show that cation-modified BC has a high capacity to remove P from aqueous solutions and then release it to plants (Li et al., 2016b; Nardis et al., 2020; Yao et al., 2013). Phosphorus sorption mechanisms by biochar are related to electrostatic attraction, precipitation (Al, Fe, Mg and Ca), ligand exchange and metallic complexation (Li et al., 2016b). The metallic complexation is formed from the interaction of oxygen-functional groups and metals as Al and Fe, which are abundant cations in tropical soils (Peng et al., 2019). Furthermore, metallic complexation can also reduce the Al activity that is toxic to plants (Lin et al., 2018; Xia et al., 2020).

Pyrolysis temperature has an impact on the pH of BC and oxygen-functional groups. The lower is the pyrolysis temperature the lower is the pH (mainly in eucalyptus sawdust BC) (Domingues et al., 2017) and the higher is the CEC of the BC (Banik et al., 2018). For the use of BC in a phosphate fertilizer composite, a higher CEC might be important to decrease the phosphate adsorption on soil surface by competition with anionic functional groups (Jiang et al., 2015), which increase P availability. Another important aspect is that BC acts as buffering agent for soil pH causing higher P availability in the soil zone surrounding OMP fertilizer (fertosphere) (Borges et al., 2020; Janke et al., 2019).

The isolated use of BC as a fertilizer composite or combined with synthetic polymers has the potential to improve physical features to fertilizer matrix, such as recalcitrance and porosity. The recalcitrance reduces the structural degradation of soluble fertilizers (granules), allowing greater stability of the matrix over time, while the porosity controls the water flow in the fertilizer matrix, reflecting directly on the release profile of the nutrients. For example, Kim et al. (2014) produced biochar pellets impregnated with K, P and different lignin contents and observed that K or P release kinetics were substantially reduced due to the stability/durability of the pellets that had the lowest specific surface area, lowest porous volume and small pores (25 nm). In another study, the N release rate from encapsulated urea with different BCs and polymer concentrations was observed to have a lower N release by granules with fewer pores on the surface (Chen et al., 2018). Thus, BC with low porosity and small pores can be an interesting composite to reduce the release profile of soluble fertilizers, which are characteristics of wood BC produced at low temperatures (Igalavithana et al., 2017; Shaheen et al., 2019).

The physical features of the granules vary according to the composite addition dose to the soluble fertilizer, which results in granules with distinct release profiles (Chen et al., 2018; Kim et al., 2014). Thereby, the evaluation of potential slow-release fertilizers requires detailed physical-chemical characterization to understand the key factors that control the release mechanism.

The evaluation of the agronomic performance is essential to consolidate the potential of biochar-based fertilizers. Recent studies show that the agronomic effectiveness of biochar-based phosphate fertilizers is similar or better than soluble phosphate fertilizers (Lustosa Filho et al., 2020, 2019, 2017; Santos et al., 2019). However, the authors mixed the phosphate sources with biomass and pyrolyzed the mixture, which changes the P forms when compared with the original P fertilizer. In another study, sugarcane straw biochar was exposed to KOH and H_3PO_4 followed by thermal activation at 600 °C and showed promising results in tropical Oxisols of contrasting textures (Borges et al., 2020). However, a detailed study focusing on the use of BC as a P fertilizer composite that could be easily adapted to P fertilizers industries and in soils of contrasting P buffering capacity is still missing.

Therefore, the objective with this study was to produce and characterize a biochar-based organomineral phosphate fertilizer and evaluate its agronomic effectiveness with a soluble mineral phosphate fertilizer (TSP). We hypothesized that organomineral phosphate fertilizer (OMP) presents greater agronomic effectiveness compared to TSP in soil with high P buffering capacity due to BC forming a barrier that reduces the P release kinetics and also by reducing P contact with the soil in the fertosphere.

2. Material and methods

2.1. Preparation of the BC and fertilizers

Wood chips (2.0 × 1.5 × 0.7 cm) (*Eucalyptus* spp.) were oven-dried at 105 °C until constant mass and then pyrolyzed in a top-opening muffle furnace as detailed elsewhere (Lustosa Filho et al., 2017). The pyrolysis temperature was raised to 350 °C at a heating rate of 10 °C min^{-1} and holding time of 1 h. The pyrolysis conditions were based on previous studies, aiming to produce small pores and preserve oxygen-functional groups (Al-Wabel et al., 2013; Keiluweit et al., 2010; Lawrinenko and Laird, 2015; Yuan et al., 2014). BC samples were ground in a disc mill and passed through a 90 μm sieve.

Fertilizers were prepared combining powdered BC with powdered triple superphosphate fertilizer [TSP- $Ca(H_2PO_4)_2$, commercial source], which were granulated (3.36–4.00 mm) using a rotating granulator. The granulation system and procedure are detailed in the supplementary material (Fig. S1). BC fertilizers were obtained by blending (B) or coating (C) TSP with BC in three proportions (5, 15 and 25% of BC, w/w), named B5, B15 and B25 for the blended ones, and C5, C15 and C25 for the coated ones (Fig. S2). Moreover, powdered TSP was granulated as a control. Granules were oven-dried at 60 °C until constant weight and subsequently characterized.

2.2. Characterization of the BC and fertilizers

Total elemental analysis of TSP was measured by Inductively Coupled Plasma with Optical Emission Spectrometry (ICP-OES, Spectro

Blue, Spectro Analytical Instruments, Germany), after nitric-perchloric acid digestion (Frazão et al., 2019). Total, water-soluble and neutral ammonium citrate plus water P in the fertilizers were also measured according to the methods described by the Brazilian Ministry of Agriculture and detailed by Lustosa Filho et al. (2019).

Total elemental analysis of the biochars was determined after ashing for 8 h at 500 °C in a muffle furnace, followed by concentrated nitric acid (HNO_3, about 65%) digestion at 120 °C and hydrogen peroxide (H_2O_2, about 35%) addition in the final digestion step (Enders and Lehmann, 2012). Then the digested material was dissolved in 20 mL of concentrated hydrochloric acid (HCl, about 37%) solution (5%, v/v) using sonication and elements contents were measured by ICP-OES (Table 1). All chemical reagents were obtained from Sigma-Aldrich (Milwaukee, WI).

Electrical conductivity (EC) and pH were measured in a S70 SevenMulti of Mettler Toledo Columbus OH, previously calibrated with standard solutions, after mixing 1.0 g of BC in 20 mL of deionized water and shaking the mixture for 1.5 h in an orbital shaker (Rajkovich et al., 2012; Zhao et al., 2013). The cation exchange capacity (CEC) of BC was determined by the ammonium acetate method (Song and Guo, 2012). Elemental analysis (C, H, N, S) was measured by elemental analyzer (model Vario TOC cube, Elementar, Germany) and the O content was calculated by mass balance [O% = 100 − (C + H + N + ash)]. The P sorption capacity (isotherm) of the BC was also evaluated. The specific surface area (SAA), porous volume (PV) and average pore size (PS) were obtained by N_2 adsorption (77.3 K) (Quantachrome, NOVA 2200e), being the BC in powder form and the fertilizers as granules. Briefly, samples (~0.3 g) were degassed with carrier gas (He) (6 h) and vacuum (6 h) at 200 °C. SSA was estimated by the BET model (Brunauer et al., 1938) and assumed multipoint plot at the range of 0.05–0.30 of partial pressure (P/P_0). The PV was obtained at 0.99 of P/P_0 and PS was obtained by desorption isotherm (0.99–0.50 of P/P_0), both calculated by the BJH model (Barrett et al., 1951).

Fourier transform infrared spectroscopy using attenuated total reflectance (FTIR/ATR) (Jasco Spectrometer, model FT/IR-4100) was obtained at wavenumber ranging from 4000 to 500 cm^{-1} with a resolution of 4 cm^{-1} and 256 scans. Only BC, TSP, B5, B15 and B25 were analyzed in powder form. The coated fertilizers were not analyzed assuming they present similar features of BC.

Table 1
Ultimate analysis and physicochemical features of wood biochar and triple superphosphate (TSP) (mean value ± standard deviation).

Feature	TSP	Biochar
C (%)	–	72.2 ± 0.01
H (%)	–	3.53 ± 0.04
N (%)	–	1.06 ± 0.01
O (%)	–	20.4 ± 0.06
S (%)	–	0.04 ± 0.01
Ash (%)	–	1.50 ± 0.04
pH	–	5.07 ± 0.02
EC (dS m^{-1}) at 25 °C[a]	–	0.17 ± 0.01
CEC ($cmol_c$ kg^{-1})[b]	–	128 ± 14.6
SSA (m^2 g^{-1})[c]	–	2.68 ± 0.11
PV(mm^3 g^{-1})[d]	–	7.23 ± 0.40
PS (nm)[e]	–	4.35 ± 0.03
K (g kg^{-1})	0.59 ± 0.06	2.87 ± 0.38
Ca (g kg^{-1})	165 ± 5.24	2.15 ± 0.14
P (g kg^{-1})	206 ± 1.80	0.95 ± 0.06
Fe (g kg^{-1})	19.4 ± 0.79	0.47 ± 0.05
S (g kg^{-1})	11.8 ± 0.54	0.10 ± 0.04
Mg (g kg^{-1})	2.89 ± 0.14	0.45 ± 0.03

[a] Electric conductivity.
[b] Cations exchange capacity.
[c] Specific surface area.
[d] Porous volume.
[e] Average pore size; averages from 6 repetitions (n = 6), except SSA, PV, PS and elementary analysis (n = 2).

Crystalline phases of BC, TSP and blended fertilizers (B5, B15 and B25) were investigated by X-ray diffraction (XRD), using a Shimadzu XRD-6000 with graphite crystal as a monochromator to select Cu-Kα_1 radiation ($\lambda = 1.5406$ Å) and 0.02°2θ s^{-1} step, adopting the scanning angle range from 5 to 70° 2θ. Scanning electron microscopy (SEM, JEOL JSM-6010LA) was also performed to observe the morphology of the coated (C25) and blended fertilizers (B25) before and after the kinetic experiment.

2.3. Kinetics experiment

A kinetics experiment was performed in a continuous stirred-flow system (Benício et al., 2017) with a flow rate of 1 mL min^{-1} using deionized water at 20 °C. Fig. S3 shows an illustration of the system. For all kinetic runs, a mass of 6 mg of P (based on P total) in the form of granules was added to the reactor (14 mL), then the water flow was actioned and the effluent was collected every 2 min for 4 h. The P concentration in effluent was measured by the molybdenum blue method (Braga and Defelipo, 1974). Korsmeyer-Peppas model (Eq. (1)) was adopted and kinetics data were fitted until the first 60% of the release curve ($M_t/M_\infty \leq 60\%$, see Eq. (1)) (Bortolin et al., 2013; Korsmeyer et al., 1983; Peppas and Sahlin, 1989; Ritger and Peppas, 1987a, 1987b).

$$\frac{M_t}{M_\infty} = kt^n \quad (1)$$

in which M_t is the amount of P release at time t, M_∞ is total amount of P inside the reactor, k is the diffusional constant of the system and n is the diffusional exponent of the release mechanism, which is driven by diffusion Fickian or swelling/relaxation of the fertilizer matrix or by both processes (Korsmeyer et al., 1983; Peppas and Sahlin, 1989; Ritger and Peppas, 1987a, 1987b).

2.4. Greenhouse experiment

Two crops were cultivated in sequence aiming to evaluate the agronomic performances of TSP and OMP fertilizer in the short- and medium-terms. The OMP fertilizer that released P more slowly was selected for the greenhouse experiment. Millet (*Pennisetum glaucum* (L.) R.Br.) was grown for 60 days, being succeeded by maize (*Zea mayz* L.) for further 30 days, in an experiment carried out under greenhouse conditions in Viçosa, Minas Gerais, Brazil (20°45′37″ S and 42°52′04″ W, 648 m altitude). A complete randomized block design in a factorial scheme 2 × 2 × 5 with four replications was employed, being two soils of contrasting P buffering capacities (Table 2), two P sources (TSP and OMP) and five P doses (0, 20, 40, 80 and 120 mg kg^{-1}, based on total P).

The soils used were two Oxisols, a clayey soil (Viçosa, Minas Gerais state, Brazil) and a sandy-loam soil (Três Marias, Minas Gerais state, Brazil) (Table 2). The soils were collected from a top layer (5–20 cm), air-dried, sieved (<4 mm) and placed into plastic bags. Sub-samples from each soil were used for chemical (Donagema et al., 2011), particle-size (Bouyoucos, 1926) and mineralogical (XRD) analyses (Table 2 and Fig. S4). Soil acidity was corrected using a mixture of $CaCO_3$ (0.8 g kg^{-1}) and $MgCO_3$ (0.2 g kg^{-1}) at a 3:1 Ca:Mg molar ratio (Vargas et al., 2019; Holland et al., 2018) and moistened to 80–90% of maximum soil water holding capacity (based on previous tests) and water was replaced weekly by weighing. After 14 days of incubation, soils were air-dried, sieved again (<4 mm) and placed into plastic pots (17 × 12 × 6 cm) of 1.0 kg. Granular P fertilizers were applied at 3 cm deep and millet was sown (20 plants/pot were maintained).

A nutrient solution that provided N, K, S, Zn, Mn, Fe, Cu, B, Mo and Ni at doses of 75, 50, 15, 4, 4, 1.55, 1.33, 0.81, 0.15 and 0.15 mg kg^{-1}, respectively, was applied to ensure adequate fertility conditions for plants growth in greenhouse experiments (Novais et al., 1991). Soil moisture was kept at 80% of water retention capacity by weight and replaced

Table 2
Physicochemical features of the original soils used in the greenhouse trial.

Characteristics	Clayey	Sandy
pH_{H2O}[a]	5.2	4.9
P (mg dm^{-3})[b]	0.7	0.1
K (mg dm^{-3})[b]	7	15
Ca ($cmol_c$ dm^{-3})[c]	0.7	0.4
Mg ($cmol_c$ dm^{-3})[c]	0.02	0.03
CEC ($cmol_c$ dm^{-3})[d]	3.97	2.49
OM (g kg^{-1})[e]	16.6	10.1
P_{rem} (mg L^{-1})[f]	11.5	32.4
Sand (g kg^{-1})[1/]	350	790
Silt (g kg^{-1})[2/]	30	20
Clay (g kg^{-1})[3/]	620	190
Textural class[4/]	Clay	Sandy-loam
Bulk density (g cm^{-3})	1.05	1.13

[a] pH soil:water ratio (1:2.5).
[b] Mehlich-1extractor.
[c] KCl extractor (1.0 mol L^{-1}).
[d] CEC = cations exchange capacity at pH 7.
[e] OM = organic matter (Walkley-Black method).
[f] P_{rem} = P remaining, refers to the soil P buffering capacity (Rogeri et al., 2016).
[1/] Sand 2.00–0.05 mm.
[2/] 0.05 > .Silt >0.002 mm.
[3/] Clay <0.002 mm.
[4/] USDA Triangular Textural Diagram.

daily. Fertilization with N, K and S at doses of 75, 50 and 12 mg kg^{-1}, respectively, was carried out at 15, 30 and 45 days after sowing. Shoots were harvested (6 cm above ground) at 60 days after sowing and were oven-dried (65 °C for ~72 h), weighed, milled and digested by nitric-perchloric acid solution (4:1, v/v, HNO_3 65% and $HClO_4$ 70%) and P content was measured by the molybdenum blue method (Braga and Defelipo, 1974). P accumulated in shoots (Pacc) was calculated by multiplying the shoot dry matter yield (SDM) by P content, while P recovery index (Prec) was calculated as described by Eq. (2) (Benício et al., 2017).

$$P_{rec}(\%) = \frac{(P_{acc-t} - P_{acc-c})}{P_{app}} \times 100 \quad (2)$$

in which P_{rec} is the fraction of P applied that is recovery by plants, $P_{acc\text{-}t}$ is the P accumulated (mg pot^{-1}) in the plant tissue at treatment$_i$, $P_{acc\text{-}c}$ is the P accumulated (mg pot^{-1}) in the plant tissue at the control treatment (without P addition) and P_{app} is the amount of P applied as fertilizer (mg kg^{-1}).

At the second crop cycle six maize seeds (BM 709 biomax) were sown in each pot. Additional fertilization with a nutrient solution containing N, K and S (75, 50 and 12 mg kg^{-1}) was applied at sowing and reapplied at 15 days after germination. Water replacement was performed daily as for the first crop and shoots were harvest at 30 days after germination and the same post-harvest procedure for millet was adopted.

2.5. Statistical analyses

The data were subjected to analysis of variance (two-way ANOVA, $\alpha = 5\%$) using R software (R core Team, 2018) and adopting ExpDes package (Ferreira et al., 2013). The means (P sources × soil) were compared by the Tukey test ($\alpha = 5\%$) and P doses by regression analysis.

3. Results and discussion

3.1. Physico-chemical analysis

Wood BC showed K, Ca and P as the main plant nutrients, which were poor as compared with other nutrient-rich feedstocks (Domingues et al., 2017) and also due to the low pyrolysis temperature that concentrate less nutrients as compared with high pyrolysis temperature (Li et al., 2017). BC presented an acidic reaction in water (pH 5.07), 128 $cmol_c$ kg^{-1} of CEC, 2.7 m^2 g^{-1} of SSA, average pore size of 4.4 nm, O/C (hydrophilic index) and (O + N)/C (polarity index) of 0.28 and 0.29, respectively (Table 1). The hydrophilic and polarity indexes suggest that BC is hydrophilic and presents charge asymmetry (polarity) (Shaheen et al., 2019), which indicates the presence of carboxylic acids and explains the acidity and high CEC found (Keiluweit et al., 2010; Song and Guo, 2012). Furthermore, the low SSA and small pore sizes of the BC are key characteristics that may reduce the interaction between water and soluble fertilizers associated with BC (Kim et al., 2014). These results are common for wood BC produced at low temperatures (Igalavithana et al., 2017; Keiluweit et al., 2010; Laghari et al., 2016; Shaheen et al., 2019).

The gradual increase of BC to TSP decreased the P content due to the dilution effect. Nevertheless, there were no clear trends for SSA, PV and PS (Table 3). Apparently, gradual BC addition increased the SSA and PV, except for B15 and C15, which present lower values. Therefore, the dose of 15% BC promotes granules denser and less porous. The physical characteristics of fertilizers are key to affect release kinetic patterns, as later discussed in the Kinetics experiment section. For instance, Kim et al. (2014) pointed out that a reduction in SSA, PV and PS contributed to slower release of nutrients from pellets that containing the same amount of biochar.

3.2. FTIR and XRD analyzes

FTIR spectra are shown in Fig. 1. Biochar presents typical signatures of stretching vibrations of O—H free (3615 cm^{-1}), indicating phenol or alcohol functional groups, and presents also stretching of O—H with H-bond (broad band centered at 3400 cm^{-1}), which is related to phenol or alcohol, carboxyl and water (Keiluweit et al., 2010). N—H stretching can also occur at 3400 cm^{-1}, which is unlikely due to the low N content of the feedstock. The three bands at 2961, 2924 and 2864 cm^{-1} are attributed to C—H stretching vibrations and indicate aliphatic compounds.

A weak band at 2659 cm^{-1} indicate O—H stretching of carboxyl groups (COOH) that are reaffirmed by stretching of C═O bond at 1695 cm^{-1} (Song et al., 2019). The carboxyl groups are common in BC surface prepared at low temperatures (Keiluweit et al., 2010) because oxygen is not drastically removed by pyrolysis (Al-Wabel et al., 2013), as verified by elemental analysis (Table 1). These oxygen-containing groups are primarily responsible for the negative charges on BC surface, favoring the complexation of Al or Fe, reducing the activity these cations and, consequently, improving the radicular environment around the fertilizer granule (Li et al., 2016b; Lin et al., 2018; Peng et al., 2019; Xia et al., 2020). In addition, thermal decomposition of lignin and cellulose contained in the wood biomass promote the formation of ketones (C═O stretching at 1440 cm^{-1}), phenols (δ O—H at 1375 and ν O—H at 3615 cm^{-1}) and guaiacyl monomers (ν C—O at 1252, 1186 and 1033 cm^{-1}) (Keiluweit et al., 2010; Song et al., 2019).

The C═C stretching at 1590 cm^{-1} correspond to aromatic compounds, which are confirmed by out of plane C—H vibrations at 871, 818 and 758 cm^{-1} (Keiluweit et al., 2010; Song et al., 2019). In BC, protonation of aromatic compounds can promote considerable anion exchange capacity (AEC), which is more evident when the pH of the medium is below of the pK_a of aromatic compounds (~5.2) (Lawrinenko and Laird, 2015). In this sense, these compounds can be interesting for BC to interact with phosphate anion into the acid environment, such as soil or acid fertilizers. Although AEC has not been measured in this work, a phosphate adsorption isotherm confirmed that BC did not demonstrate P adsorption capacity (data not shown), most likely due to its high CEC and also due to the isotherm pH (6.0) being above of the pK_a of aromatic compounds (Lawrinenko and Laird, 2015; Shaheen et al., 2019).

The FTIR spectrum of TSP (Fig. 1) show absorption bands of water molecule (ν O—H at 3461 and 3242 cm^{-1}), including structural water of the crystal (δ O—H at 1650 and ρ O—H 662 cm^{-1}) (Nasri et al.,

Table 3
Physicochemical characteristics for fertilizer granules prepared with different biochar (BC) ratios.

Features	TSP	B5	B15	B25	C5	C15	C25
P_{toltal} (%)	20.6 ± 0.2	19.9 ± 0.1	18.1 ± 0.2	15.4 ± 0.4	19.7 ± 0.5	18.8 ± 0.3	15.5 ± 0.2
P_{water} (%)	17.7 ± 0.3	15.6 ± 0.2	14.0 ± 0.3	12.6 ± 0.5	15.6 ± 0.4	13.9 ± 0.3	12.7 ± 0.2
P_{NAC} (%)[a]	18.9 ± 0.3	18.6 ± 0.2	16.6 ± 0.2	14.6 ± 0.4	18.9 ± 0.6	16.7 ± 0.5	14.3 ± 0.3
SSA ($m^2\ g^{-1}$)[b]	1.1 ± 0.1	1.1 ± 0.1	0.8 ± 0.1	1.9 ± 0.1	1.1 ± 0.1	1.0 ± 0.1	2.0 ± 0.1
PV ($mm^3\ g^{-1}$)[c]	3.1 ± 0.1	3.3 ± 0.4	2.3 ± 0.3	5.2 ± 0.1	3.0 ± 0.1	2.7 ± 0.2	5.0 ± 0.2
PS (nm)[d]	4.0 ± 0.1	4.4 ± 0.1	4.5 ± 0.1	5.0 ± 0.1	5.0 ± 0.1	4.4 ± 0.1	4.4 ± 0.1

Note: BC fertilizers were obtained from the blending (B) or coating (C) of TSP with BC in three weight proportions (5, 15 and 25% of BC), resulting in the materials named as B5, B15 and B25 for the blended materials and C5, C15 and C25 for the coated materials.
[a] P soluble in neutral ammonium citrate plus water (P contents, mean value ± standard deviation, n = 6).
[b] Specific surface area (n = 2).
[c] Porous volume (n = 2).
[d] Average pore size (n = 2).

2014). The absorption bands of stretching vibrations of O—H groups (ν O—H) in $H_2PO_2^-$ occurs at 2491, 2337 and 1650 cm^{-1} (Boonchom, 2009), but only the first is evident (Fig. 1) because of the atmospheric CO_2 absorption bands (~2340 cm^{-1}) (Sheng et al., 2018) and the water molecule (δ OH 1650 cm^{-1}) that coexist on the same region of the others bands (Boonchom, 2009). Furthermore, the phosphate groups (Fig. 1) contained in TSP were observed at 1234 (δ P-O-H), 1078 (ν_{as} PO_2^- - asymmetric stretching), 954 (ν_{as} $P(OH)_2$), 888 (out of plane P-O-H bending), 861 (ν_s $P(OH)_2$ - symmetric stretching), 568 (δ PO_2^-) and 506 cm^{-1} (ρ PO_2^-) (Boonchom, 2009; Nasri et al., 2014). As expected, OMP fertilizers display similar absorption bands of the TSP (Fig. 1), which is the main component of such fertilizers. Nevertheless, B25 shows the BC signatures due to its high concentration (25% w/w).

The X-ray diffraction patterns of the materials are shown in supplementary material (Fig. S4). No crystalline phases were detected for BC, while TSP and BC fertilizers showed peaks that were attributed to monocalcium phosphate hydrate ($Ca(H_2PO_4)_2 \cdot H_2O$), dicalcium pyrophosphate tetrahydrate ($Ca_2P_2O_7 \cdot 4H_2O$), garronite ($Ca_3(Si,Al)_{16}O_{32} \cdot 13H_2O$), iron hydrogen phosphate hydrate ($Fe_3H_9(PO_4)_6 \cdot 6H_2O$) and fluorapatite ($Ca_5(PO_4)_3F$). Such XRD patterns are close to those of the standard powder diffraction files (PDF), corresponding to the cards 009-0347, 044-0762, 016-0905, 044-0812 and 01-071-0881, respectively. The composition of TSP is due to its parent rock material (Charanworapan et al., 2013) and industrial process (Nasri et al., 2014) that generate high solubility P compounds.

3.3. Kinetics of P release

Phosphorus release profiles and kinetics parameters for the fertilizers are shown in Fig. 2. Most minerals contained in TSP are water soluble and only a small part (~6% of the total P) are low solubility phases (Charanworapan et al., 2013; Nasri et al., 2014), such as garronite, fluorapatite and iron phosphate minerals. After 1.5 h of water flow, the fertilizers TSP, B5, B15, B25, C5, C15 and C25 released 92, 85, 82, 79, 49, 30 and 31% of the total P, respectively. After 4 h the same fertilizers accumulated the releasing of 94, 94, 93, 92, 83, 74 and 72% of the total P.

The increase of BC ratios to TSP gradually reduced the P release rate as observed by the decreasing *k* values, especially for coating, but C15 and C25 showed similar *k* values, that is, their kinetic profiles are similar (Fig. 2). According to Korsmeyer-Peppas model (Ritger and Peppas, 1987b) the parameter *n* indicate the release mechanism and for values between 0.50 and 1.0 combines the diffusion process and the swelling/relaxation of the fertilizer matrix, while *n* values higher than 1.0 indicate swelling/relaxation as the main release mechanism. Therefore, TSP, B5, B15 and B25 are controlled by diffusion and swelling/relaxation mechanisms, while C5, C15 and C25 are mainly controlled by swelling/

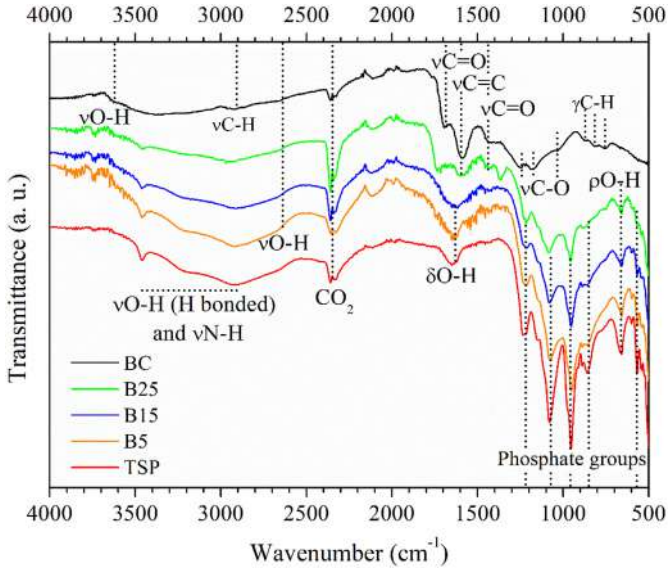

Fig. 1. FTIR spectra of biochar (BC), triple superphosphate (TSP), TSP with 25, 15 and 5 g (w/w) of BC (B25, B15 and B5, respectively). Vibrational modes: ν – stretching, δ – bending, ρ -rocking and γ – out of plane deformations. Phosphate groups: P-O-H, PO_2^- and $P(OH)_2$.

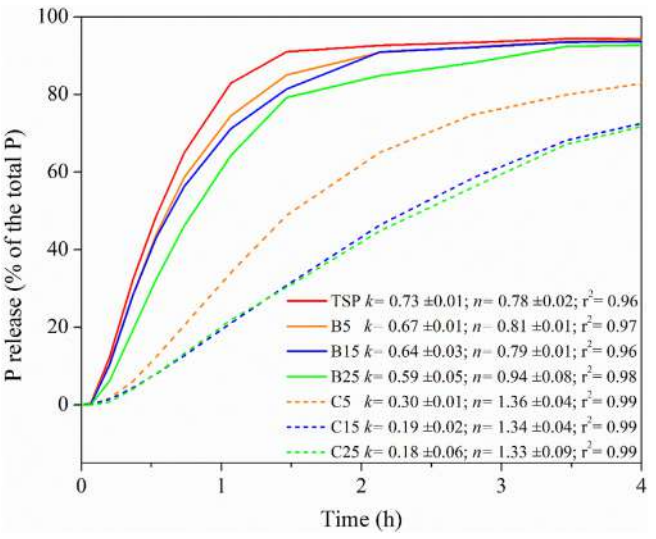

Fig. 2. Kinetics profiles of P release and parameters *k* and *n* for the fertilizers synthetized (see Eq. (1), mean value ±standard deviation, n = 3). Triple superphosphate (TSP), blend of TSP with biochar (BC) at the weight proportions of 5, 15 and 25% (B5, B15 and B25, respectively) and coating of TSP with BC (C5, C15 and C25).

relaxation mechanisms, which indicate a greater participation of the fertilizer matrix on P release and show that BC coating has more effect than blending on reducing the P release rate.

Based on kinetics modelling approach and SEM images, we suggest that firstly water interacts with TSP encrusted on the surface of the blended granule (Fig. 3h) and then P quickly diffuses toward the less concentrated medium (Korsmeyer et al., 1983; Peppas and Sahlin, 1989; Ritger and Peppas, 1987a, 1987b). Secondly, TSP dissolution promotes the formation of channels on the surface (Fig. 3b) and galleries into the fertilizer matrix (Fig. 3c), facilitating the evolution of the hydration front and consequently the diffusion process. The first and second moments represent the initial portion of the release curve (Fig. 2). Finally, the amount of P remaining into the matrix is slowly released due to the physical protection of the BC pores network (Dias et al., 2018). For coated OMP fertilizers, the water flow removes aliphatic compounds (hydrophobicity) on BC surface, increasing its affinity for water (Das and Sarmah, 2015). Then, the water interacts with hydrophilic groups causing a swelling of the coating that acquires a new arrangement (swelling/relaxation), which controls the water flow between the inside and outside of the fertilizer core (Dias et al., 2018).

As a result of this release mechanism, the C15 and C25 coated fertilizers showed the same kinetic profiles, which suggests that the rate of 15% BC is sufficient to control the P release. Moreover, from the point of view of fertilizer production, this result is economically advantageous because it uses lower BC content and allows the production of a more concentrated OMP fertilizer. Therefore, C15 OMP fertilizer was selected for the greenhouse experiment.

3.4. Greenhouse experiment

The results of ANOVA shows that fertilizers sources and P doses applied in the distinct soils affected plant responses in both

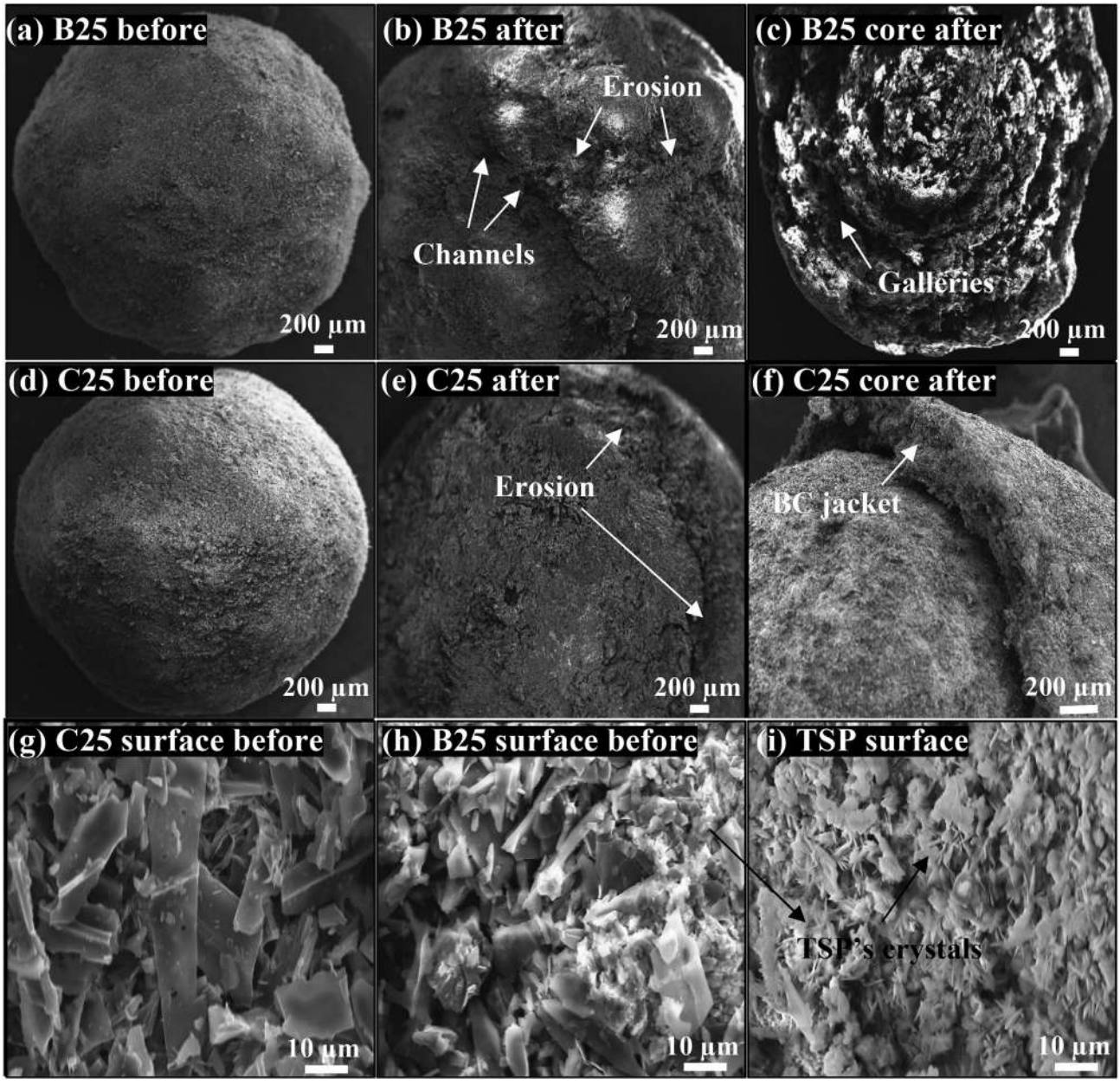

Fig. 3. SEM images of (a) B25 fertilizer before kinetics test (4 h) (magnification of 50×), (b) B25 after test (70×), (c) B25 cross section after (60×), (d) C25 before (50×), (e) C25 after (80×), (f) C25 cross section after (70×), (g) C25 surface before (3500×), (h) B25 surface before (3500×) and (i) granular triple superphosphate surface (TS) (3500×).

cultivations ($p < 0.05$) (Table S1). Shoot dry matter mass, P accumulated and P recovery rate in both crops are shown in Figs. 4 and 5. Regardless of the P source or crops cycle, the biomass yield was higher in P-fertilized plots when compared with control (without P) due to very low available P in both of soils (0.7 and 0.1 mg kg^{-1} in Mehlich-1 for clayey and sandy soils, respectively) (Table 2). As for millet, shoot dry matter mass (Figs. 4a and S6) and P accumulated (Fig. 4c) increased, while P recovery decreased (Fig. 4e) with increasing P rates in both soils. Phosphorus recovery decrease because the gradual P addition surpass the plant uptake rate and most P contained in the soil solution is adsorbed over time by the soil solid phase and becomes unavailable to plants (Vance et al., 2003).

Shoot dry matter mass, P accumulated and P recovery indicated greater yield and P uptake of plants cultivated in the clayey soil as compared with the sandy soil (Fig. 4a, c and e). Usually, clay Oxisol with high P buffering capacity (lower remaining P, Table 2) maintain lower P concentration into the soil solution as compared with sandy soils (higher remaining P), which causes plants to adopt strategies to enhance P acquisition, such as increasing root surface area (Vance et al., 2003). Such root adaptation also increases water absorption and hence higher nutrients uptake, which are key factors for increased shoot dry matter mass, P accumulated and, consequently, P recovery. The better root yield in the clay soil is one of the processes that explain the better plant performance for this soil (Frazão et al., 2019; Vance et al., 2003).

There was effect of P sources ($p > 0.05$) only in the clayey soil, which showed 10% and 20% better performance for P accumulated and P recovery in clayey soil, respectively, when compared to TSP (Fig. 5a). However, despite the higher P recovery from C15 fertilizer (Fig. 4e), shoot dry matter mass was similar for both fertilizers, as observed by similar *c* values from Mitscherlich equation (Fig. 4a). Such effect is a physiological response of plants to adapt to P poor soils by improving nutrient use efficiency, i.e., to produce more shoot dry matter mass with less P (Vance et al., 2003).

This means that OMP (C15) allows a significant reduction of P applied without yield loss, which can lower the cost of production and allow a greater P use sustainability. These results indicate that the slow-release biochar-based organomineral fertilizer (C15) was more effective for P supply to plants in the high P buffering capacity clay soil when compared with the conventional fertilizer (TSP). The fast P release from TSP causes a fast saturation to the soil solution and P is sorbed to the soil solid phase becoming unavailable to plants over time (Benício et al., 2017). Conversely, the coating of BC (C15) prevent the direct contact of P with the soil and displays a slow-release pattern (Fig. 2), making P more available over time and favoring plant uptake (better synchronization with plant demand) (Geng et al., 2015). Moreover, organic compounds can reduce P adsorption by the soil and decrease the toxic Al content. Nevertheless, this effect is limited to a small area around the granule (Fink et al., 2016; Lin et al., 2018; Xia et al., 2020). Additionally, the negative charges of the BC can prevent the Al incursion to the TSP core, reducing the Al—P precipitation.

As for maize (Fig. S7), shoot dry matter mass and P accumulated showed a small increase with increasing P doses (Fig. 4b and d), demonstrating a small residual effect for both fertilizers ($p < 0.05$). Phosphorus recovery was not influenced by P doses, but it was influenced by the soil type (Fig. 4f). Higher P recovery was obtained in sand soil (2.93%) when compared to clayey soil (1.95%) ($p < 0.05$). Since the sandy soil has a lower P buffering capacity than the clayey soil, an increased plant P uptake and consequently higher P recovery in the sandy soil was expected, especially in the second crop cycle, in which there was a greater contact time of P fertilizer with soils. Despite these differences between the soils, P recovery in both soils was low, as well as for the first crop (19.9% and 22.4% for the sandy and clayey soil, respectively). Moreover, for maize the P sources did not influence the yield, P accumulated and P recovery.

The P sources did not differ from each other ($p < 0.05$), regardless of the soil type (Fig. 5c and d). As observed in the first cultivation, there was higher P accumulated and P recovery when plants were cultivation in treated clayey soil C15 with increase 12% and 27%, respectively, when compared with TSP. This increase uptake and P recovery reflected only in a slight increase of 4.5% in shoot dry matter mass. Based on these observations, we confirm our hypothesis that combining BC with soluble P-fertilizers would enhance P recovery in clayey soil, therefore, improving the P use efficiency in soil with high P fixation capacity. Differences in P recovery among these P sources might be related to their different solubility. The TSP has approximately 86% of the P_{total} water-soluble, whereas in C15 it is about 73%. In agreement with our results, (Frazão et al., 2019), using a clayey Oxisol, found that organomineral, which is a derivative of the mixture of poultry litter and TSP, is as effective as conventional water-soluble P fertilizers like TSP. In contrast, unlike our study, in sandy soils (Entisol), water-soluble P fertilizer was better than organomineral.

After the second harvest the soil pH was measured (data not shown), but it was not influenced by any of the treatments. This result was expected because TSP does not substantially alter the soil pH (Benício et al., 2017) and the BC had a pH of 5.07 (Table 1), which is close to the pH of the original soils (Table 2) (Dai et al., 2017).

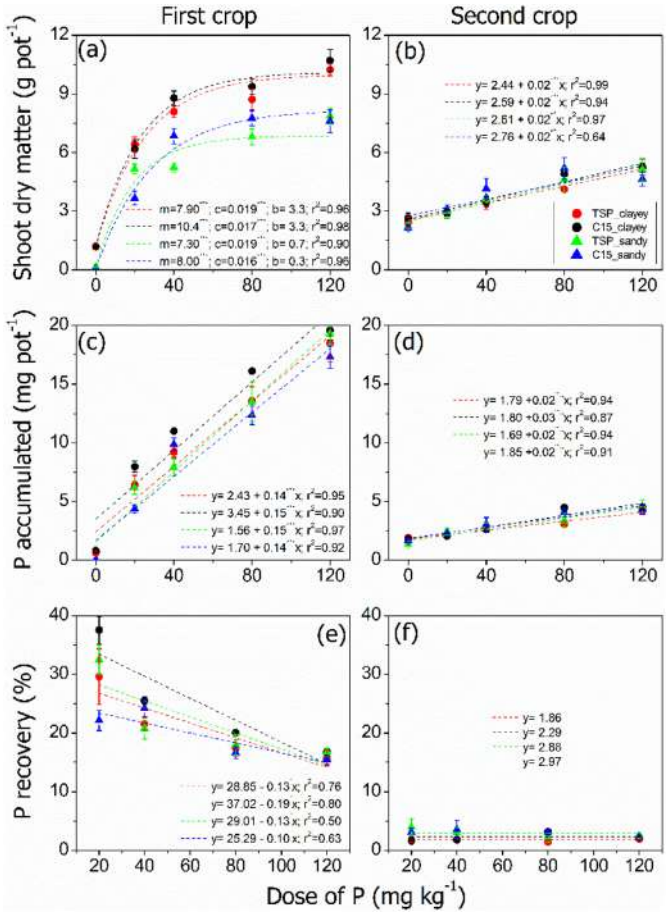

Fig. 4. Shoot dry matter, P accumulated and P recovery in first crop (millet) and second crop (maize). Plants were grown in different Oxisols (clayey and sandy), P sources (TSP - triple superphosphate or C15 - TSP coated with 15% of biochar) and at different P rates. The parameters *m*, *c* and *b* (a) are of the Mitscherlich equation $\left(\hat{y} = m\left[1-10^{-c(x+b)}\right]\right)$, which *m* is maximum yield for the range experimental, the parameter *c* indicates relative effectiveness of the P sources and *b* indicates the P derived from the soil plus

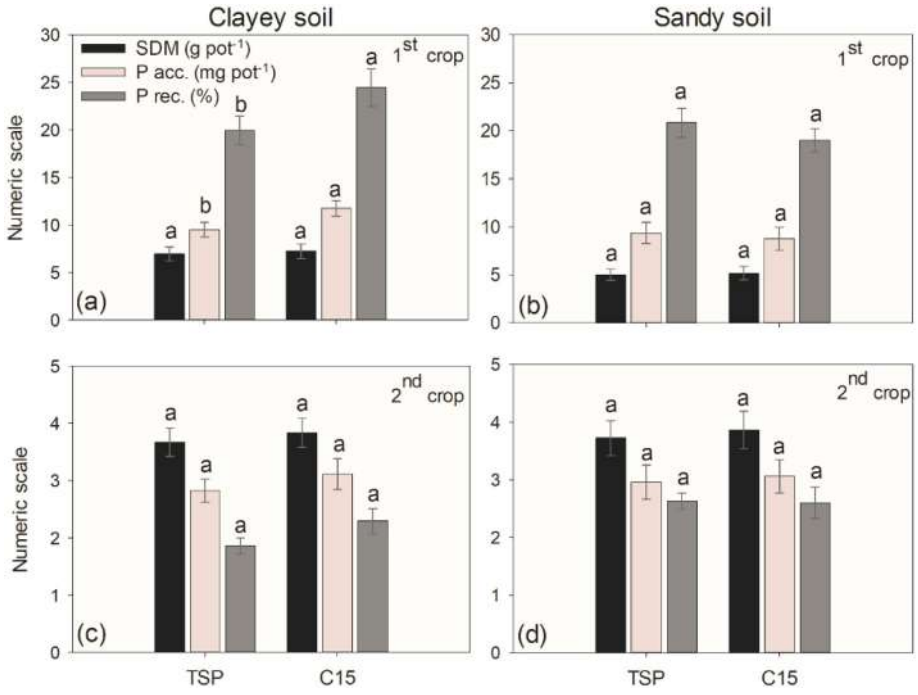

Fig. 5. Shoot dry matter mass average (SDM), P accumulated (P acc.) and recovery (P rec.) by plants in the first crop (millet) and second crop (maize). Plants were grown on clayey or sandy soil, further fertilized with two different granular P sources (TSP - triple superphosphate or C15, that is, TSP coated with 15% of biochar). Different letters on same color bars charts show differences between P sources (Tukey test, $p < 0.05$). Bars denote the standard error.

4. Conclusions

Organomineral phosphate fertilizer (OMP) presented a slower-release kinetics for P when compared with soluble mineral fertilizer (triple superphosphate-TSP). The lower P release of OMP is due to the physical protection of P by the organic matrix (biochar-BC). When OMP is produced as a blended fertilizer, the control of P release is less effective and it is controlled by the diffusion and swelling/relaxation mechanisms. On the other hand, when OMP is produced using the organic matrix as a coating material, the control over P release is stronger and controlled mostly by the swelling/relaxation mechanism.

In the first crop cycle, the soil application of OMP (coated with 15% BC) provided positive impacts on the P uptake and P recovery, especially in the clayey soil. As the coating technology had a better control over P release, it lowered the contact time of P with the clay oxides and also represented a barrier (high CEC) for the cations to go into the fertilizer granules and precipitate with P, increasing its availability. However, these effects are ephemeral and were only noticeable in the first crop cycle, which lasted for 60 days. In the second crop cycle, P sources (OMP and TSP) did not differ from each other.

Therefore, wood-based biochar showed potential as a fertilizer composite to improve the fertilizer effectiveness as P source in highly weathered tropical soils. In terms of practical aspects, the same material applied at the same ratio can have different effects on the behavior of the P release from the fertilizer. Understanding this behavior will allow one to produce fertilizers designed to solve specific problems in the field.

CRediT authorship contribution statement

Denison Pogorzelski: Conceptualization, Methodology, Formal analysis, Investigation, Writing - original draft, Writing - review & editing.**José Ferreira Lustosa Filho:**Writing - review & editing.**Patrícia Cardoso Matias:**Methodology, Writing - original draft.**Wedisson Oliveira Santos:**Methodology, Writing - original draft.**Leonardus Vergütz:**Conceptualization, Methodology, Resources, Writing - review & editing, Supervision, Project administration, Funding acquisition.**Leônidas Carrijo Azevedo Melo:**Conceptualization, Methodology, Validation, Writing - review & editing, Supervision.

Declaration of competing interest

The authors declare that they have no known competing financial interests or personal relationships that could have appeared to influence the work reported in this paper.

Acknowledgments

The authors are grateful Jefferson Santana da Silva Carneiro for his assistance with the graphical abstract.This study was financed in part by the Coordenação de Aperfeiçoamento de Pessoal de Nível Superior - Brasil (CAPES) - Finance Code 001.

Appendix A. Supplementary data

Supplementary Information regarding granules of the fertilizers synthetized (Figs. S1 and S2); Scheme of the stirred-flow system and reactor parts (Fig. S3); XRD patterns of the biochar, TSP, TSP with 25, 15 and 5% of BC (B25, B15 and B5, respectively) and C15 fertilizer after the two crops (Fig. S4); XRD patterns of the clay fraction (natural) for the soils used in the greenhouse trial (Fig. S5); Visualization of the millet plants grown (30 days after sowing) in each treatment (Fig. S6); Visualization of the maize plants grown (30 days after sowing) in each treatment (Fig. S7) and Summary of variance analysis (Table S1) can be found in the online version. Supplementary data to this article can be found online at https://doi.org/10.1016/j.scitotenv.2020.140604.

References

Al-Wabel, M.I., Al-Omran, A., El-Naggar, A.H., Nadeem, M., Usman, A.R.A., 2013. Pyrolysis temperature induced changes in characteristics and chemical composition of biochar

produced from conocarpus wastes. Bioresour. Technol. 131, 374–379. https://doi.org/10.1016/j.biortech.2012.12.165.
Banik, C., Lawrinenko, M., Bakshi, S., Laird, D.A., 2018. Impact of pyrolysis temperature and feedstock on surface charge and functional group chemistry of biochars. J. Environ. Qual. 47, 452–461. https://doi.org/10.2134/jeq2017.11.0432.
Barrett, E.P., Joyner, L.G., Halenda, P.P., 1951. The determination of pore volume and area distributions in porous substances. I. Computations from nitrogen isotherms. J. Am. Chem. Soc. 73, 373–380. https://doi.org/10.1021/ja01145a126.
Baveye, P.C., 2015. Looming scarcity of phosphate rock and intensification of soil phosphorus research. Rev. Bras. Ciência do Solo 39, 637–642. https://doi.org/10.1590/01000683rbcs20140819.
Benício, L.P.F., Constantino, V.R.L., Pinto, F.G., Vergütz, L., Tronto, J., da Costa, L.M., 2017. Layered double hydroxides: new technology in phosphate fertilizers based on nanostructured materials. ACS Sustain. Chem. Eng. 5, 399–409. https://doi.org/10.1021/acssuschemeng.6b01784.
Boonchom, B., 2009. Parallelogram-like microparticles of calcium dihydrogen phosphate monohydrate (Ca(H2PO4)2·H2O) obtained by a rapid precipitation route in aqueous and acetone media. J. Alloys Compd. 482, 199–202. https://doi.org/10.1016/j.jallcom.2009.03.157.
Borges, B.M.M.N., Strauss, M., Camelo, P.A., Sohi, S.P., Franco, H.C.J., 2020. Re-use of sugarcane residue as a novel biochar fertiliser - increased phosphorus use efficiency and plant yield. J. Clean. Prod. 262, 121406. https://doi.org/10.1016/j.jclepro.2020.121406.
Bortolin, A., Aouada, F.A., Mattoso, L.H.C., Ribeiro, C., 2013. Nanocomposite PAAm/methyl cellulose/montmorillonite hydrogel: evidence of synergistic effects for the slow release of fertilizers. J. Agric. Food Chem. 61, 7431–7439. https://doi.org/10.1021/jf401273n.
Bouyoucos, G.J., 1926. Estimation of the colloidal material in soils. Science (80-.) 64, 362–364. https://doi.org/10.1126/science.64.1658.362.
Braga, J.M., Defelipo, B.V., 1974. Determinação espectrofotométrica de fósforo em extratos de solos e plantas. Rev. Ceres 21, 73–85.
Brunauer, S., Emmett, P.H., Teller, E., 1938. Adsorption of gases in multimolecular layers. J. Am. Chem. Soc. 60, 309–319. https://doi.org/10.1021/ja01269a023.
Calabi-Floody, M., Medina, J., Rumpel, C., Condron, L.M., Hernandez, M., Dumont, M., Mora, M. de la L., 2018. Smart fertilizers as a strategy for sustainable agriculture. Advances in Agronomy, 1st ed Elsevier Inc https://doi.org/10.1016/bs.agron.2017.10.003.
Campos, M., Antonangelo, J.A., Alleoni, L.R.F., 2016. Phosphorus sorption index in humid tropical soils. Soil Tillage Res. 156, 110–118. https://doi.org/10.1016/j.still.2015.09.020.
Charanworapan, C., Suddhiprakarn, A., Kheoruenromne, I., Wiriyakitnateekul, W., Gilkes, R.J., 2013. An evaluation of three Thai phosphate rocks for agronomic use based upon their chemical and mineralogical properties. Soil Sci. Plant Nutr. 59, 522–534. https://doi.org/10.1080/00380768.2013.810546.
Chen, S., Yang, M., Ba, C., Yu, S., Jiang, Y., Zou, H., Zhang, Y., 2018. Preparation and characterization of slow-release fertilizer encapsulated by biochar-based waterborne copolymers. Sci. Total Environ. 615, 431–437. https://doi.org/10.1016/j.scitotenv.2017.09.209.
Dai, Z., Zhang, X., Tang, C., Muhammad, N., Wu, J., Brookes, P.C., Xu, J., 2017. Potential role of biochars in decreasing soil acidification - a critical review. Sci. Total Environ. 581–582, 601–611. https://doi.org/10.1016/j.scitotenv.2016.12.169.
Das, O., Sarmah, A.K., 2015. The love–hate relationship of pyrolysis biochar and water: a perspective. Sci. Total Environ. 512–513, 682–685. https://doi.org/10.1016/j.scitotenv.2015.01.061.
Dias, D.S., Crespi, M.S., Torquato, L.D.M., Kobelnik, M., Ribeiro, C.A., 2018. Torrefied banana tree fiber pellets having embedded urea for agricultural use. J. Therm. Anal. Calorim. 131, 705–712. https://doi.org/10.1007/s10973-016-6049-7.
Domingues, R.R., Trugilho, P.F., Silva, C.A., Melo, I.C.N.A. de, Melo, L.C.A., Magriotis, Z.M., Sánchez-Monedero, M.A., 2017. Properties of biochar derived from wood and high-nutrient biomasses with the aim of agronomic and environmental benefits. PLoS One 12, e0176884. https://doi.org/10.1371/journal.pone.0176884.
Donagema, G.K., Campos, D.V.B. de, Calderano, S.B., Teixeira, W.G., Viana, J.H.M., 2011. Manual de métodos de análise de solo. 2 edição. (Rio de Janeiro).
Enders, A., Lehmann, J., 2012. Comparison of wet-digestion and dry-ashing methods for total elemental analysis of biochar. Commun. Soil Sci. Plant Anal. 43, 1042–1052. https://doi.org/10.1080/00103624.2012.656167.
Ferreira, E.B., Cavalcanti, P.P., Nogueira, D.A., 2013. ExpDes: Experimental Designs Package. R Package Version 1.1.2.
Fink, J.R., Inda, A.V., Tiecher, T., Barrón, V., 2016. Iron oxides and organic matter on soil phosphorus availability. Ciência e Agrotecnologia 40, 369–379. https://doi.org/10.1590/1413-70542016404023016.
Frazão, J.J., Benites, V. de M., Ribeiro, J.V.S., Pierobon, V.M., Lavres, J., 2019. Agronomic effectiveness of a granular poultry litter-derived organomineral phosphate fertilizer in tropical soils: soil phosphorus fractionation and plant responses. Geoderma 337, 582–593. https://doi.org/10.1016/j.geoderma.2018.10.003.
Geng, J., Ma, Q., Zhang, M., Li, C., Liu, Z., Lyu, X., Zheng, W., 2015. Synchronized relationships between nitrogen release of controlled release nitrogen fertilizers and nitrogen requirements of cotton. F. Crop. Res. 184, 9–16. https://doi.org/10.1016/j.fcr.2015.09.001.
Gérard, F., 2016. Clay minerals, iron/aluminum oxides, and their contribution to phosphate sorption in soils—a myth revisited. Geoderma 262, 213–226. https://doi.org/10.1016/j.geoderma.2015.08.036.
Gilbert, N., 2009. The disappearing nutrient. Nature 461, 716–718. https://doi.org/10.1038/461716a.
Holland, J.E., Bennett, A.E., Newton, A.C., White, P.J., McKenzie, B.M., George, T.S., Pakeman, R.J., Bailey, J.S., Fornara, D.A., Hayes, R.C., 2018. Liming impacts on soils, crops and biodiversity in the UK: a review. Sci. Total Environ. 610–611, 316–332. https://doi.org/10.1016/j.scitotenv.2017.08.020.
Igalavithana, A.D., Mandal, S., Niazi, N.K., Vithanage, M., Parikh, S.J., Mukome, F.N.D., Rizwan, M., Oleszczuk, P., Al-Wabel, M., Bolan, N., Tsang, D.C.W., Kim, K.-H., Ok, Y.S., 2017. Advances and future directions of biochar characterization methods and applications. Crit. Rev. Environ. Sci. Technol. 47, 2275–2330. https://doi.org/10.1080/10643389.2017.1421844.
Janke, C.K., Fujinuma, R., Moody, P., Bell, M.J., 2019. Biochemical effects of banding limit the benefits of nitrification inhibition and controlled-release technology in the fertosphere of high N-input systems. Soil Res 57, 28–40. https://doi.org/10.1071/SR18211.
Jeffery, S., Abalos, D., Prodana, M., Bastos, A.C., van Groenigen, J.W., Hungate, B.A., Verheijen, F., 2017. Biochar boosts tropical but not temperate crop yields. Environ. Res. Lett. 12, 053001. https://doi.org/10.1088/1748-9326/aa67bd.
Jiang, J., Yuan, M., Xu, R., Bish, D.L., 2015. Mobilization of phosphate in variable-charge soils amended with biochars derived from crop straws. Soil Tillage Res. 146, 139–147. https://doi.org/10.1016/j.still.2014.10.009.
Jiang, D., Chu, B., Amano, Y., Machida, M., 2018. Removal and recovery of phosphate from water by Mg-laden biochar: batch and column studies. Colloids Surfaces A Physicochem. Eng. Asp. 558, 429–437. https://doi.org/10.1016/j.colsurfa.2018.09.016.
Keiluweit, M., Nico, P.S., Johnson, M.G., Kleber, M., 2010. Dynamic molecular structure of plant biomass-derived black carbon (biochar). Environ. Sci. Technol. 44, 1247–1253. https://doi.org/10.1021/es9031419.
Kim, P., Hensley, D., Labbé, N., 2014. Nutrient release from switchgrass-derived biochar pellets embedded with fertilizers. Geoderma 232–234, 341–351. https://doi.org/10.1016/j.geoderma.2014.05.017.
Korsmeyer, R.W., Gurny, R., Doelker, E., Buri, P., Peppas, N.A., 1983. Mechanisms of solute release from porous hydrophilic polymers. Int. J. Pharm. 15, 25–35. https://doi.org/10.1016/0378-5173(83)90064-9.
Laghari, M., Naidu, R., Xiao, B., Hu, Z., Mirjat, M.S., Hu, M., Kandhro, M.N., Chen, Z., Guo, D., Jogi, Q., Abudi, Z.N., Fazal, S., 2016. Recent developments in biochar as an effective tool for agricultural soil management: a review. J. Sci. Food Agric. 96, 4840–4849. https://doi.org/10.1002/jsfa.7753.
Lawrinenko, M., Laird, D.A., 2015. Anion exchange capacity of biochar. Green Chem. 17, 4628–4636. https://doi.org/10.1039/C5GC00828J.
Lehmann, J., Joseph, S., 2015. Biochar for Environmental Management: Science, Technology and Implementation. 2nd ed. Routledge, London.
Li, R., Wang, J.J., Zhou, B., Awasthi, M.K., Ali, A., Zhang, Z., Gaston, L.A., Lahori, A.H., Mahar, A., 2016a. Enhancing phosphate adsorption by Mg/Al layered double hydroxide functionalized biochar with different Mg/Al ratios. Sci. Total Environ. 559, 121–129. https://doi.org/10.1016/j.scitotenv.2016.03.151.
Li, R., Wang, J.J., Zhou, B., Awasthi, M.K., Ali, A., Zhang, Z., Lahori, A.H., Mahar, A., 2016b. Recovery of phosphate from aqueous solution by magnesium oxide decorated magnetic biochar and its potential as phosphate-based fertilizer substitute. Bioresour. Technol. 215, 209–214. https://doi.org/10.1016/j.biortech.2016.02.125.
Li, H., Dong, X., da Silva, E.B., de Oliveira, L.M., Chen, Y., Ma, L.Q., 2017. Mechanisms of metal sorption by biochars: biochar characteristics and modifications. Chemosphere 178, 466–478. https://doi.org/10.1016/j.chemosphere.2017.03.072.
Lin, Q., Zhang, L., Riaz, M., Zhang, M., Xia, H., Lv, B., Jiang, C., 2018. Assessing the potential of biochar and aged biochar to alleviate aluminum toxicity in an acid soil for achieving cabbage productivity. Ecotoxicol. Environ. Saf. 161, 290–295. https://doi.org/10.1016/j.ecoenv.2018.06.010.
Lora, E.S., Andrade, R.V., 2009. Biomass as energy source in Brazil. Renew. Sust. Energ. Rev. 13, 777–788. https://doi.org/10.1016/j.rser.2007.12.004.
Lustosa Filho, J.F., Penido, E.S., Castro, P.P., Silva, C.A., Melo, L.C.A., 2017. Co-pyrolysis of poultry litter and phosphate and magnesium generates alternative slow-release fertilizer suitable for tropical soils. ACS Sustain. Chem. Eng. 5, 9043–9052. https://doi.org/10.1021/acssuschemeng.7b01935.
Lustosa Filho, J.F., Barbosa, C.F., Carneiro, J.S. da S., Melo, L.C.A., 2019. Diffusion and phosphorus solubility of biochar-based fertilizer: visualization, chemical assessment and availability to plants. Soil Tillage Res. 194, 104298. https://doi.org/10.1016/j.still.2019.104298.
Lustosa Filho, J.F., Carneiro, J.S. da S., Barbosa, C.F., de Lima, K.P., Leite, A. do A., Melo, L.C.A., 2020. Aging of biochar-based fertilizers in soil: effects on phosphorus pools and availability to Urochloa brizantha grass. Sci. Total Environ. 709, 136028. https://doi.org/10.1016/j.scitotenv.2019.136028.
Nardis, B.O., Santana Da Silva Carneiro, J., Souza, I.M.G. de, Barros, R.G. de, Azevedo Melo, L.C., 2020. Phosphorus recovery using magnesium-enriched biochar and its potential use as fertilizer. Arch. Agron. Soil Sci. 00, 1–17. https://doi.org/10.1080/03650340.2020.1771699.
Nasri, K., Chtara, C., Hassen, C., Fiallo, M., Sharrock, P., Nzihou, A., El Feki, H., 2014. Recrystallization of industrial triple super phosphate powder. Ind. Eng. Chem. Res. 53, 14446–14450. https://doi.org/10.1021/ie502033j.
Novais, R.F., Neves, J.C.L., Barros, N.F., 1991. Ensaio em ambiente controlado. In: Oliveira, A.J., Garrido, W.E., Araújo, J.D., Lourenço, S. (Eds.), Métodos de Pesquisa Em Fertilidade Do Solo. Embrapa-SEA, Brasília, pp. 189–253.
Novais, S.V., Zenero, M.D.O., Barreto, M.S.C., Montes, C.R., Cerri, C.E.P., 2018. Phosphorus removal from eutrophic water using modified biochar. Sci. Total Environ. 633, 825–835. https://doi.org/10.1016/j.scitotenv.2018.03.246.
Novak, J.M., Busscher, W.J., Laird, D.L., Ahmedna, M., Watts, D.W., Niandou, M.A.S., 2009. Impact of biochar amendment on fertility of a southeastern coastal plain soil. Soil Sci. 174, 105–112. https://doi.org/10.1097/SS.0b013e3181981d9a.
Peng, Y., Sun, Y., Sun, R., Zhou, Y., Tsang, D.C.W., Chen, Q., 2019. Optimizing the synthesis of Fe/Al (Hydr)oxides-biochars to maximize phosphate removal via response surface model. J. Clean. Prod. 237, 117770. https://doi.org/10.1016/j.jclepro.2019.117770.

Peppas, N.A., Sahlin, J.J., 1989. A simple equation for the description of solute release. III. Coupling of diffusion and relaxation. Int. J. Pharm. 57, 169–172. https://doi.org/10.1016/0378-5173(89)90306-2.

R core Team, 2018. R: A Language and Environment for Statistical Computing.

Rajkovich, S., Enders, A., Hanley, K., Hyland, C., Zimmerman, A.R., Lehmann, J., 2012. Corn growth and nitrogen nutrition after additions of biochars with varying properties to a temperate soil. Biol. Fertil. Soils 48, 271–284. https://doi.org/10.1007/s00374-011-0624-7.

Ritger, P.L., Peppas, N.A., 1987a. A simple equation for description of solute release I. Fickian and non-Fickian release from non-swellable devices in the form of slabs, spheres, cylinders or discs. J. Control. Release 5, 23–36. https://doi.org/10.1016/0168-3659(87)90034-4.

Ritger, P.L., Peppas, N.A., 1987b. A simple equation for description of solute release II. Fickian and anomalous release from swellable devices. J. Control. Release 5, 37–42. https://doi.org/10.1016/0168-3659(87)90035-6.

Rogeri, D.A., Gianello, C., Bortolon, L., Amorim, M.B., 2016. Substitution of clay content for P-remaining as an index of the phosphorus buffering capacity for soils of Rio Grande Do Sul. Rev. Bras. Cienc. do Solo 40, 1–14. https://doi.org/10.1590/18069657rbcs20140535.

Roy, E.D., Richards, P.D., Martinelli, L.A., Coletta, L. Della, Lins, S.R.M., Vazquez, F.F., Willig, E., Spera, S.A., VanWey, L.K., Porder, S., 2016. The phosphorus cost of agricultural intensification in the tropics. Nat. Plants 2, 16043. https://doi.org/10.1038/nplants.2016.43.

Roy, E.D., Willig, E., Richards, P.D., Martinelli, L.A., Vazquez, F.F., Pegorini, L., Spera, S.A., Porder, S., 2017. Soil phosphorus sorption capacity after three decades of intensive fertilization in Mato Grosso, Brazil. Agric. Ecosyst. Environ. 249, 206–214. https://doi.org/10.1016/j.agee.2017.08.004.

Santos, S.R. dos, Lustosa Filho, J.F., Vergütz, L., Melo, L.C.A., 2019. Biochar association with phosphate fertilizer and its influence on phosphorus use efficiency by maize. Ciência e Agrotecnologia 43, e025718. https://doi.org/10.1590/1413-7054201943025718.

Shaheen, S.M., Niazi, N.K., Hassan, N.E.E., Bibi, I., Wang, H., Tsang, D.C.W., Ok, Y.S., Bolan, N., Rinklebe, J., 2019. Wood-based biochar for the removal of potentially toxic elements in water and wastewater: a critical review. Int. Mater. Rev. 64, 216–247. https://doi.org/10.1080/09506608.2018.1473096.

Sheng, H., Oh, M.H., Osowiecki, W.T., Kim, W., Alivisatos, A.P., Frei, H., 2018. Carbon dioxide dimer radical anion as surface intermediate of photoinduced CO2 reduction at aqueous cu and CdSe nanoparticle catalysts by rapid-scan FT-IR spectroscopy. J. Am. Chem. Soc. 140, 4363–4371. https://doi.org/10.1021/jacs.8b00271.

Song, W., Guo, M., 2012. Quality variations of poultry litter biochar generated at different pyrolysis temperatures. J. Anal. Appl. Pyrolysis 94, 138–145. https://doi.org/10.1016/j.jaap.2011.11.018.

Song, B., Chen, M., Zhao, L., Qiu, H., Cao, X., 2019. Physicochemical property and colloidal stability of micron- and nano-particle biochar derived from a variety of feedstock sources. Sci. Total Environ. 661, 685–695. https://doi.org/10.1016/j.scitotenv.2019.01.193.

Vance, C.P., Uhde-Stone, C., Allan, D.L., 2003. Phosphorus acquisition and use: critical adaptations by plants for securing a nonrenewable resource. New Phytol. 157, 423–447. https://doi.org/10.1046/j.1469-8137.2003.00695.x.

Vargas, J.P.R., dos Santos, D.R., Bastos, M.C., Schaefer, G., Parisi, P.B., 2019. Application forms and types of soil acidity corrective: changes in depth chemical attributes in long term period experiment. Soil Tillage Res. 185, 47–60. https://doi.org/10.1016/j.still.2018.08.014.

Vikrant, K., Kim, K.-H., Ok, Y.S., Tsang, D.C.W., Tsang, Y.F., Giri, B.S., Singh, R.S., 2018. Engineered/designer biochar for the removal of phosphate in water and wastewater. Sci. Total Environ. 616–617, 1242–1260. https://doi.org/10.1016/j.scitotenv.2017.10.193.

Withers, P.J.A., Elser, J.J., Hilton, J., Ohtake, H., Schipper, W.J., van Dijk, K.C., 2015. Greening the global phosphorus cycle: how green chemistry can help achieve planetary P sustainability. Green Chem. 17, 2087–2099. https://doi.org/10.1039/C4GC02445A.

Xia, H., Riaz, M., Zhang, M., Liu, B., El-Desouki, Z., Jiang, C., 2020. Biochar increases nitrogen use efficiency of maize by relieving aluminum toxicity and improving soil quality in acidic soil. Ecotoxicol. Environ. Saf. 196, 110531. https://doi.org/10.1016/j.ecoenv.2020.110531.

Yao, Y., Gao, B., Chen, J., Yang, L., 2013. Engineered biochar reclaiming phosphate from aqueous solutions: mechanisms and potential application as a slow-release fertilizer. Environ. Sci. Technol. 47, 8700–8708. https://doi.org/10.1021/es4012977.

Yuan, H., Lu, T., Wang, Y., Huang, H., Chen, Y., 2014. Influence of pyrolysis temperature and holding time on properties of biochar derived from medicinal herb (radix isatidis) residue and its effect on soil CO2 emission. J. Anal. Appl. Pyrolysis 110, 277–284. https://doi.org/10.1016/j.jaap.2014.09.016.

Zhao, L., Cao, X., Mašek, O., Zimmerman, A., 2013. Heterogeneity of biochar properties as a function of feedstock sources and production temperatures. J. Hazard. Mater. 256–257, 1–9. https://doi.org/10.1016/j.jhazmat.2013.04.015.